Intrinsic optical bistability in a cavity

Michael Scalora and Joseph W. Haus
Department of Physics, Rensselaer Polytechnic Institute, Troy, New York 12180

Charles M. Bowden
Research Directorate, U.S. Army Missile Command, Redstone Arsenal, Alabama 35898-5248
(Received 12 June 1989; revised manuscript received 23 January 1990)

Absorptive, dispersive, and diffractive effects are studied in a nonlinear ring-cavity configuration containing an intrinsically bistable medium modeled generically by a nonlinear oscillator. The output intensity is shown to exhibit steady-state and periodic characteristics for constant input intensity, but no chaotic solutions are found. We find that the plane-wave analysis is inconsistent with the inclusion of diffraction effects and that periodic output characteristics are affected even for Fresnel numbers of order 1000. Our results are contrasted with previously reported experimental and theoretical work.

I. INTRODUCTION

Under suitable conditions, electromagnetic waves propagating through a ring cavity containing a nonlinear medium can cause the output from the cavity to exhibit bistable behavior. For a given nonlinear medium the bistable characteristics can be controlled by the input intensity, the laser detuning from a resonance in the nonlinear material and by the cavity detuning. Thorough theoretical investigations have been carried out both in the plane-wave limit and for waves propagating with diffractive coupling.[1-3] The numerical studies have shown that diffraction significantly changes the bistable characteristics; in fact, diffraction coupling will lower the contrast between the two stable output intensities and will change the input intensity threshold value for switching between the two output intensities.[2] Moreover, diffraction can introduce a rich variety of periodic and chaotic instabilities in the transverse structure of the output intensity.[3] When mirrors and feedback are required for the observed optical bistable characteristics, we call this manifestation of the phenomenon *extrinsic* optical bistability.

The nonlinear oscillator model has been investigated by Goldstone and Garmire[4] and, extensively, by Haus *et al.*[5] The authors show that this medium exhibits optical bistability without a cavity due to increased absorption. This phenomenon has been called *intrinsic* optical bistability because it is intrinsic and local to the material and does not require an external feedback. A study of transverse effects in this system[6] shows that bistability is not significantly altered by varying the Fresnel number down to order unity but that an interesting redistribution of the electromagnetic energy takes place due to increased diffraction and high absorption at the center of the input intensity profile. As shown in Ref. 5 the sudden absorption at some point inside the medium amounts to changing the rate at which the intensity is dissipated in the longitudinal direction. This means that a boundary has been created at that point with respect to the nonlinear index, and that, for continuity, a backward wave originates there, orders of magnitude smaller than the forward component, but nevertheless, counter propagating. This amounts to saying that the index of refraction suffers an abrupt change and that depending on the laser detuning from the atomic resonance, it may be considerable.

In this paper we will investigate wave propagation through an intrinsically bistable nonlinear medium, inside a ring cavity with plane mirrors, modeled generically by a collection of anharmonic oscillators, and will also present new results for low Fresnel numbers by propagating a Gaussian beam in the cavity. The treatment of diffraction effects in intrinsic optical bistability has not yet been the focus of extensive study for this configuration, which is required if results of future experimental observation are to be fully understood. Earlier theoretical studies of intrinsic bistable media in a cavity by Lindberg, Koch, and Haug[7] have introduced a mean-field approximation with respect to the propagation of the field in the nonlinear medium. They have also neglected dispersive effects, and have predicted unusual periodic structures, which has been qualitatively confirmed in a hybrid experiment.[8] The hybrid experiment has an electronic feedback to simulate a cavity and does not, therefore, include diffractive coupling or dispersive effects.

We stress here that the appearance of the periodic structures in Ref. 7 for a cavity with optical feedback requires that a complete description of bistability include diffraction effects, since the transverse profile can simultaneously have several periods of oscillation. That is, each intensity will correspond to a specific oscillatory regime. The question which shall be taken up later, and which is the main point addressed by the article, is then how will the beam behave due to the interaction of the rays from a Gaussian beam, where many different oscillatory periods are present at the same time. Any sharp

demarcation between the transverse oscillatory regimes will be smoothed through diffractive coupling. Further, there are quantitative aspects of the theory that are not in agreement with the hybrid experiment, which we ascribe to propagation effects; the hybrid experiment does not have the transverse instabilities that we discuss here, since they do not mix the output field with the input.

As discussed in Ref. 5, the position of the boundary in the medium which separates the two states of absorption depends on the incident intensity. This means that in a ring cavity, as the feedback is returned to the input mirror, the boundary between the high and low absorption state may shift in and out of the medium at both the entry and exit boundaries of the material. Therefore, if sharp discontinuities occur inside the medium, one cannot altogether ignore dispersive effects since the phase of the field, which intrinsically depends on the polarization, also suffers such a discontinuity.

In Ref. 7 the authors have investigated the plane-wave limit of a ring cavity with a semiconductor medium inserted into it. Although they treat a different model than in this work, both materials exhibit intrinsic optical bistability. However, there are several significant assumptions that they have introduced that we examine in this paper. We retain dispersion, diffraction, and propagation effects. Even though the bistability mechanism is induced absorption, in view of a discontinuity of the index of refraction within the medium, it is too drastic to assume a dispersion-free medium *a priori*. Further, as diffraction becomes increasingly important, coupling of the rays in the transverse direction together with possible phase discontinuity at the internal boundary, may cause effects that would otherwise go unnoticed. Even though dispersion is not as important as absorption in this system, a somewhat dispersive medium can exhibit quite different characteristic curves. For this reason we perform a detailed analysis by considering both absorptive and dispersive effects.

II. FORMALISM

The polarization of the medium is composed of two parts: the nonlinear part coming from the local response of the oscillator, and the linear part, which will contain both background modes of the polarization and a possible linear response of the oscillator at the local level. Therefore we may write for the total polarization with a constitutive relation:

$$\mathbf{P}_{\text{total}}=\mathbf{P}_{\text{NL}}+\mathbf{P}_{\text{L}}=\chi\mathbf{E} , \tag{1}$$

where $\mathbf{P}_{\text{L}}$ will contain $\mathbf{P}_b=(\epsilon_b-1)\mathbf{E}/4\pi$, the background modes. The coefficient $\chi(|\mathbf{E}|)$ is a function of the field. For intrinsic optical bistability, the field dependence is a multivalued function.

If a set of nonlinear oscillators is considered, the nonlinear susceptibility can be obtained from a constitutive relation between $\mathbf{P}$, the macroscopic polarization, and $\mathbf{E}$, the local oscillating field. A quartic Duffing potential is assumed, and the equation of motion for the polarization is

$$\frac{\partial^2}{\partial t^2}\mathbf{P}+\gamma\frac{\partial\mathbf{P}}{\partial t}=\frac{ne^2}{m}\mathbf{E}-\frac{\kappa}{m}\mathbf{P}-\frac{\beta|P|^2}{e^2mn^2}\mathbf{P} , \tag{2}$$

where γ is the damping coefficient, $\kappa/m=\omega_0^2$ is the resonant frequency, and n is the dipole density. Equation (2) gives the total response of the oscillator and as mentioned previously, it will contain both a linear and nonlinear part. Assuming that the field and the polarization are aligned along the same direction, the fields are separated into slowly varying amplitudes which have a space and time dependence of the type

$$X(\mathbf{r},t)=Y(\mathbf{r},t)e^{i(\mathbf{k}\cdot\mathbf{r}-\omega t)}+\text{c.c.} , \tag{3}$$

where $Y(\mathbf{r},t)$ is the slowly varying amplitude; to simplify our equations further, we use the following scaling of the functions:

$$\tilde{E}=\left[\frac{e^2}{\omega\gamma m}\right]\left[\frac{3\beta}{\gamma\omega me^2}\right]^{1/2}E,\quad \tilde{P}=\left[\frac{3\beta}{\gamma\omega mn^2e^2}\right]^{1/2}P . \tag{4}$$

We assume that the wave is propagating along the z axis. We write Maxwell's equation in the slowly varying envelope approximation with retarded time coordinates as

$$\frac{\partial}{\partial\zeta}\tilde{E}-\frac{i}{F}\nabla_{\perp}^2\tilde{E}=i(1+\tilde{\Delta}^2)\left[\tilde{P}-\frac{\tilde{\Delta}}{\tilde{\Delta}^2+1}\tilde{E}\right] ; \tag{5}$$

ζ is the retarded-time coordinate $z-vt$ scaled by the linear absorption coefficient of the material α so that $\zeta=\alpha(z-vt)$, v is the group velocity of the wave; $F=2\alpha kd^2$ is the absorption Fresnel number, also scaled by the width of the input beam waist d; and k is the wave number [see Eq. (9) below]. This scaling is most convenient since it leaves only one atomic parameter in Eq. (5), i.e., $\tilde{\Delta}$. For similar reasons an analogous gain length Fresnel number is defined in superfluorescence.[9] The paraxial approximation has been assumed[10] and $\nabla_{\perp}^2$ is the transverse Laplacian that includes the coupling to x and y coordinates. In our numerical results in Sec. IV we use only one transverse dimension. This can be justified by using a cavity with side walls,[11] but the use of two transverse dimensions, or cylindrical symmetry should not qualitatively alter the results. Applying the slowly varying envelope approximation to Eq. (2), and assuming steady-state conditions, Eq. (5) is then solved together with the scaled steady-state polarization equation

$$\tilde{E}=\tilde{P}(\tilde{\Delta}-i+|\tilde{P}|^2) , \tag{6}$$

where $\tilde{\Delta}=(\omega_0^2-\omega^2)/(\gamma\omega)$. In obtaining Eq. (6), it has been assumed that the material relaxation rate γ in Eq. (2) is much more rapid than the time scale on which the field in the cavity responds, which is governed by the cavity round-trip time τ_R, i.e, $\gamma\tau_R\gg1$. The susceptibility used in Eq. (1) is a useful definition for integrating Maxwell's equation in the form

$$\frac{\partial\tilde{E}}{\partial\zeta}-\frac{i}{F}\nabla_{\perp}^2\tilde{E}=-\chi(|\tilde{E}|,\zeta)\tilde{E} , \tag{7}$$

and χ is obtained from a constitutive relation which is

identified from Eqs. (6) and (7):

$$\chi=-i(1+\tilde{\Delta}^2)\{1/[(\tilde{\Delta}-i)+|\tilde{P}|^2]-\tilde{\Delta}/(1+\tilde{\Delta}^2)\} . \quad (8)$$

The wave number has been chosen so that the linear part of the field is completely removed,

$$k^2=\frac{\omega^2}{c^2}\left[\epsilon_b+\frac{\omega_p^2\Delta}{\Delta^2+(\gamma\omega)^2}\right] , \quad (9)$$

and the linear absorption is

$$\alpha=\frac{\gamma\omega^3\omega_p^2}{2kc^2[\Delta^2+(\gamma\omega)^2]} , \quad (10)$$

with $\Delta=\omega_0^2-\omega^2$, $\omega_p^2=4\pi ne^2/m$ being the plasma frequency in SI units and ϵ_b the linear part of the dielectric constant due to the ever present background modes.

In a ring cavity configuration with plane mirrors, then, the propagation equation [Eq. (7)] is supplemented by the usual boundary condition

$$E(0,x,t)=\sqrt{T}E_{\rm in}(x)+Re^{i\phi_L}E(L,x,t-\tau) , \quad (11)$$

where $E_{\rm in}(x)$ is the input field outside the cavity, T and R are entry and exit mirror transmission and reflection coefficients, $T=1-R=0.1$, ϕ_L the cavity detuning,[12] L the length of the nonlinear medium, which is taken to be 10% of the total length of the cavity throughout our discussion (in our scaling of the length $L=0.1$), and τ the time required for the field to propagate around in the cavity free space $\tau=\tau_R-L/v$. Since we are using the constitutive relations, the relaxation time of the material medium is assumed to be very small with respect to τ. The role that τ plays in the boundary condition is then to remind us that the input field must be combined with the field that left the output mirror a time τ earlier. This is properly accounted for by propagating the field at L by the remaining amount in the empty part of the cavity (L is 10% of the ring-cavity length in all our results). Therefore, our numerical solution will use Eq. (7) together with Eq. (11) in order to calculate the output field in terms of the input field. The split operator method is used to propagate a Gaussian beam, and is extensively discussed in the literature.[13,14]

In order to test our algorithm, we compare our numerical results for infinite Fresnel numbers with analytical results. The solutions for the polarization and its phase inside the medium from Ref. 5 are

$$(1+\tilde{\Delta}^2)\ln\frac{|\tilde{P}|^2}{|\tilde{P}_0|^2}+\tfrac{1}{2}(|\tilde{P}|^4-|\tilde{P}_0|^2)+4\tilde{\Delta}(|\tilde{P}|^2-|\tilde{P}_0|^2)=-2(1+\tilde{\Delta}^2)\zeta \quad (12)$$

and

$$\phi_p(\zeta)=\phi_0-\tilde{\Delta}\zeta-\tilde{\Delta}\ln\frac{|\tilde{P}|}{|\tilde{P}_0|}-\tfrac{1}{2}(|\tilde{P}|^2-|\tilde{P}_0|^2) , \quad (13)$$

where we have taken $\tilde{P}=|\tilde{P}|e^{i\phi_p(\zeta)}$. If we then define $\tilde{E}=|\tilde{E}|e^{i\phi_e(\zeta)}$, from Eq. (6) we determine

$$\phi_e(\zeta)=\phi_p(\zeta)+\tan^{-1}\left[\frac{-1}{\tilde{\Delta}+|\tilde{P}|^2}\right] . \quad (14)$$

In order to determine ϕ_0 in Eq. (13), it is useful to define the steady-state input field at the input to the medium as the complex number

$$E_0=E_{0r}+iE_{0i} . \quad (15)$$

Combining (14) and (15) we find

$$\phi_p(0)\equiv\phi_0=\tan^{-1}\left[\frac{E_{0i}}{E_{0r}}\right]-\tan^{-1}\left[\frac{-1}{\tilde{\Delta}+|\tilde{P}_0|^2}\right] . \quad (16)$$

All the elements necessary for the solution are now in place, namely, Eqs. (12)–(16); these together with the boundary condition Eq. (11) define an iterative map of the complex electric field. Our integrations of Eq. (5) ($F=\infty$) will match the analytical solution to any desired accuracy, depending on the size of our integration step $\Delta\zeta$ along the longitudinal coordinate.

III. RESULTS I: PLANE WAVE

In Fig. 1 we plot the local field intensity inside the medium as a function of the polarization density. The turning points are determined by $\tilde{\Delta}$, the laser detuning from atomic resonance, see Eq. (6), all other parameters being held fixed. As the intensity is increased above point A, the high absorption branch is suddenly reached, causing a discontinuous decrease in the output intensity from the medium. As the wave propagates inside the medium, it may be reduced below the second turning point B, which means a sudden return to the low absorption

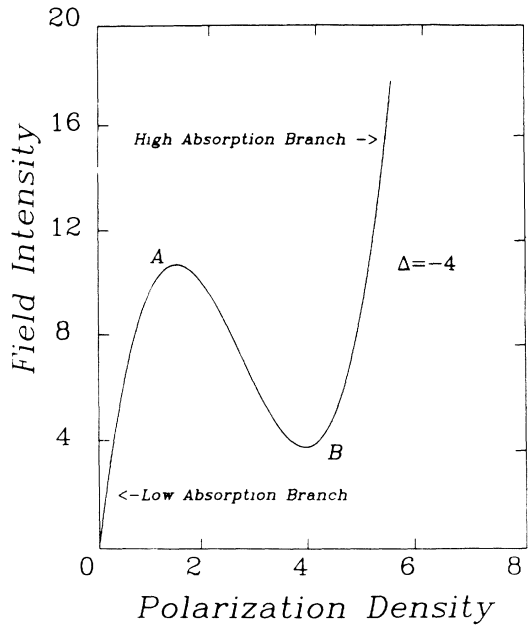

FIG. 1. Field intensity vs polarization density with $\tilde{\Delta}=-4$ inside the medium at steady state.

branch. If the input beam intensity is chosen between A and B, so that it may be closer to B, then the feedback may not be strong enough to raise the output above A; a steady-state output intensity from the cavity may quickly be achieved at some intermediate value. This is shown for two different input intensities in Figs. 2(a) and 2(b) where the output intensity is plotted as a function of time in units of the cavity round-trip time τ_R; in our integration in the medium we used 3000 steps (i.e., $\Delta\xi=\frac{1}{3}\times 10^{-4}$).

As the input beam intensity is increased further, the turning point A of Fig. 1 can be reached. In Fig. 2(c) the

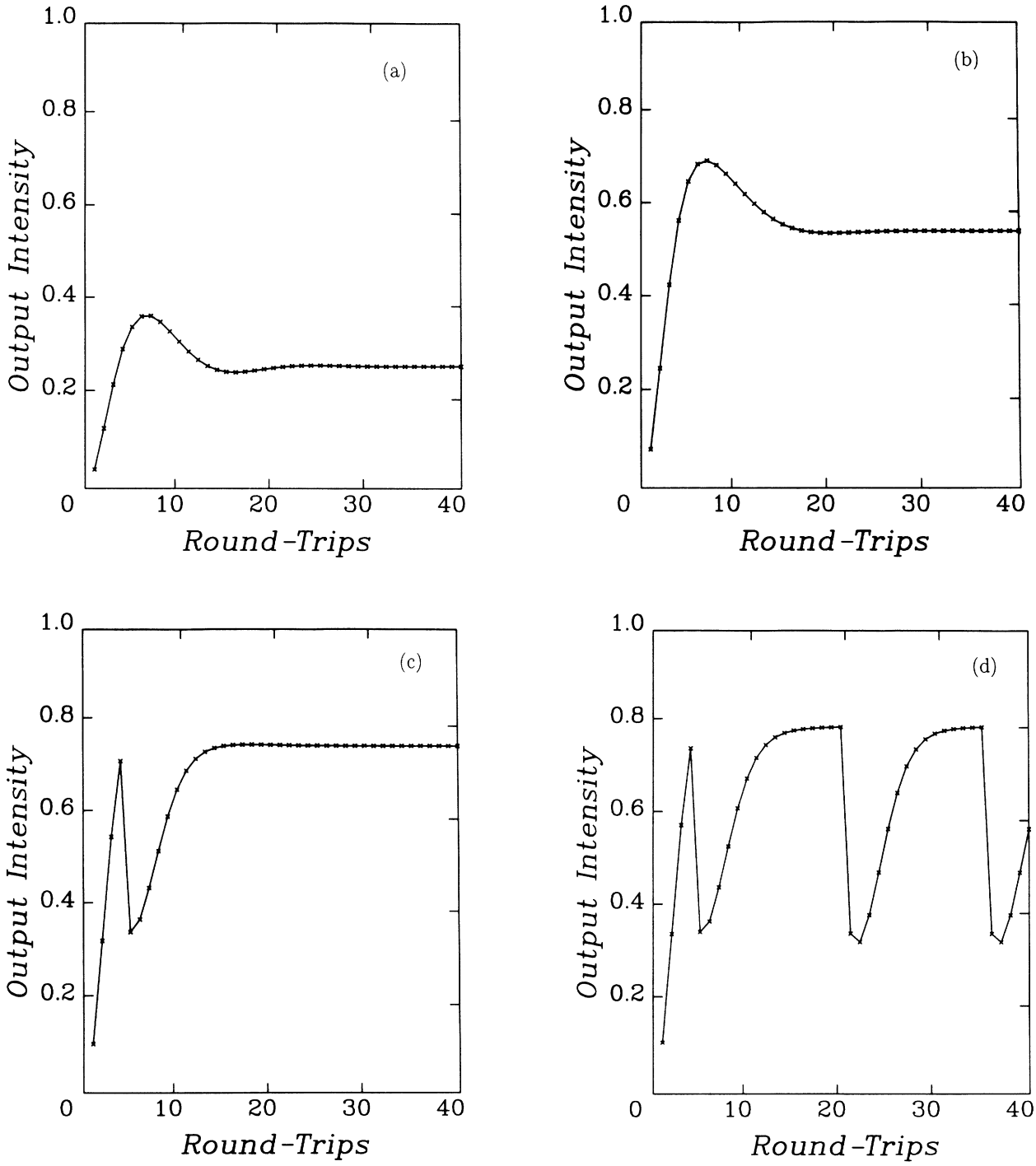

FIG. 2. Output intensity vs number of round-trips with $\bar{\Delta}=-4$ and (a) $I_{in}=5$, (b) $I_{in}=10$, (c) $I_{in}=13$, (d) $I_{in}=13.7$. Cavity detuning is $\phi_L=0.4$, $T=0.1$, and $F=\infty$.

input intensity is $I_{in}=13$. After the fourth pass around the cavity (each pass is denoted by a cross) there is a sudden drop in the output intensity and we find that for successive passes in the cavity the absorption is too strong for the system to climb above the turning point a second time, and again a steady state is eventually achieved.

As the input intensity is raised further, in Fig. 2(d) where $I_{in}=13.7$, a periodic instability develops in the output intensity. In this case ten round-trips are necessary for a complete cycle to repeat itself. Further increase of the input intensity, will, for this detuning, result in a decrease of the oscillation period. The period changes by unity at critical input field values until a steady state output is reached. For instance, we set $I_{in}=20$ in Fig. 3, and we find that this self-induced oscillation is now of period 4. We find that the range of intensities over which a certain period is stable increases with increasing intensity. Figure 4 summarizes the situation for a large range of intensities and one detuning from the oscillator resonance.

We find that over a limited range of intensities, each period of oscillation is stable. As the intensity is increased, the number of round-trips necessary to complete the loop must now be smaller due to the increased feedback. This stepping down of the period by one unit then makes sense, if we simply insure that the input intensity is varied smoothly and that the feedback adds a little to the wave each time it comes around. For this purpose, it then becomes important to preserve information on the phase of the field, and this is accomplished by a full consideration of propagation effects. A larger detuning ($\tilde{\Delta}=-8$) is shown in Fig. 5; we find overlap regions between period N and $(N-1)$, which has been interpreted as a Farey tree. This is discussed below.

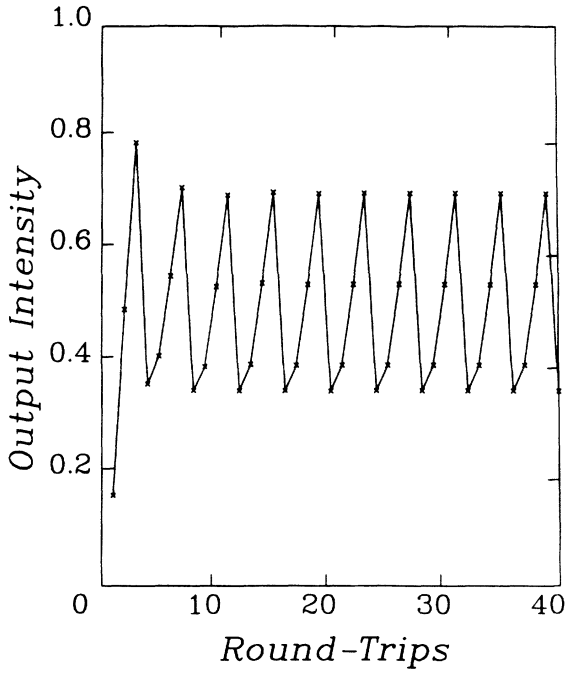

FIG. 3. Same as Fig. 2, but with $I_{in}=20$.

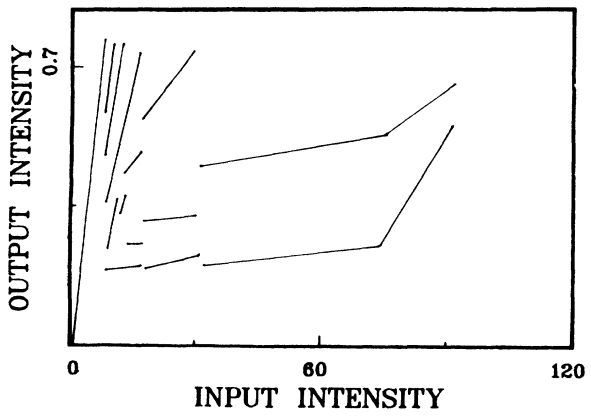

FIG. 4. Output intensity vs input intensity with $\tilde{\Delta}=-4$ and $F=\infty$.

Our results are consistent with the experimental results of Wegener and Klingshirn[8,15] and qualitatively different from what is theoretically predicted in Ref. 7. In Ref. 7, contrary to experimental results, the maximum output intensity increases as the intensity is increased, due to the neglect of propagation effects. Our model does not allow for this increase of the maximum intensity since the low absorption branch turning point determines the largest intensity that the field can have before absorption becomes high. Therefore the uppermost point can be the value of the intensity at the point B, before the medium is precipitated to the high absorption branch.

The nature of our nonlinearity, i.e., the multivalued polarization as a function of the field, offers an explanation as to why chaotic behavior has not been observed.[7,8,15] As can be seen from Eq. (6), or Fig. 1, in the low absorption branch the intensity is well approximated by a linear function of the polarization. In this regime, then, nonlinear dispersive effects cannot be observed. In the high absorption branch, far away from the turning point denoted by B, the field can be expressed as $\tilde{E}=\tilde{P}|\tilde{P}|^2$, so that the nonlinear susceptibility takes the form

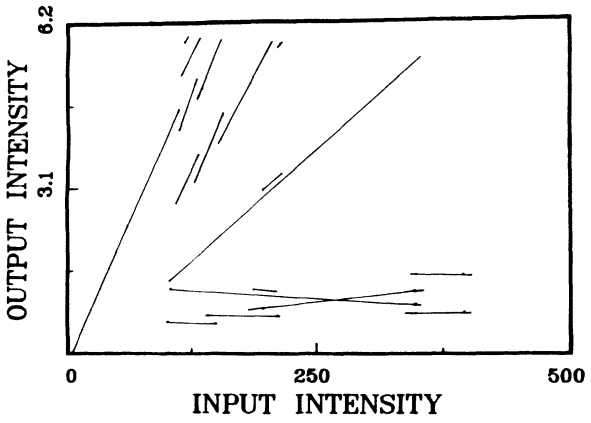

FIG. 5. Output intensity vs input intensity with $\tilde{\Delta}=-8$.

$$\chi = -i[(1+\tilde{\Delta}^2)/|\tilde{P}|^2 - \tilde{\Delta}] . \quad (17)$$

But in this limit $|\tilde{P}|^2 \gg \tilde{\Delta}$ since the second turning point B has value of order $\tilde{\Delta}$. Therefore, the first term in Eq. (17) can be neglected, leaving only the linear term in the approximation, and again no dispersive effects can be seen. The only region where nonlinear effects can occur is between the turning points A and B. But in that region $|\tilde{P}|^2 \cong \tilde{\Delta}$ so that dispersion is automatically taken out, leaving the absorption, i.e., the imaginary term, to dominate. Even if an expansion were performed in order to obtain a Kerr-medium nonlinearity, which is known to display chaos in both the dispersive and absorptive regimes,[12] it would have to apply in the region between the turning points. But contrary to a two-level atom, the oscillator dynamics gives, to lowest order, a field-dependent dispersion coefficient proportional to $L|\tilde{E}|^2/\tilde{\Delta}^4$ where L is the length of the medium, as opposed to the two-level atom dispersive coefficient, which is proportional to $L|\tilde{E}|^2/\tilde{\Delta}^2$. The expansion breaks down for $|\tilde{E}| \cong \tilde{\Delta}$; therefore, even with large detuning values, the absorption dominates. This is contrasted with two-level atomic media, where dispersive effects regain dominance away from the resonant frequency of the oscillator.

We now return to the Farey tree alluded to in Fig. 5. A Farey series for the rational numbers p/q and r/s, where p, q, r, and s are integers, is obtained by adding numerators and denominators, respectively, so that the series may be written as p/q, r/s, $(p+r)/(q+s)$, etc. The analysis in terms of a Farey tree is useful since it may be used to describe the degree of stability of an oscillating mode. This question arises when we consider an input intensity which is at the threshold of a transition from a mode of period N to one of period $(N-1)$. For example, referring to Fig. 6, we find that an intensity $I_{in}=110$ gives a stable structure of period 5; more precisely, it takes three passes to reach the higher turning point and two passes to reach the lower. We denote this as a (3,2) mode. Each period exhibits one maximum so that in this language, we may refer to the (3,2) mode as a 5/1 mode, where 5 is the period and 1 is the number of peaks displayed within that cycle. Therefore we may take the number of peaks as being an indicator of the degree of stability of that mode.

If we apply the same analysis to Fig. 7, where $I_{in}=150$, we may denote this as a (2,2) mode or, equivalently, as a 4/1 mode. If an intermediate value of the intensity is used, as in Fig. 8, we see that both the (2,2) and the (3,2) modes can coexist, giving a total period of 9, and two well-defined peaks, that is, a 9/2 mode. It is clear that 9, the new period, is obtained by adding the individual periods, and that 2 is now the total number of peaks within one cycle. This is the basis for the Farey series, and in principle, any period and number of maxima is allowed. Using the same language as in Ref. 7, we find that the structure only develops to second generation; that is, there is an intensity range where two stable oscillating modes coexist, as shown in Fig. 8.

We do not expect more than two modes to exist in those regions, since this is a boundary region where the transition takes place from oscillations of period N to those of period $N-1$. This region allows only these two modes to coexist. We note that this mode coexistence does not occur for all values of $\tilde{\Delta}$. In fact, since this dynamics is favored only by higher values of the detuning, one might be led to the belief that the mode coexistence might be a direct result of increased dispersion. As the period and the number of peaks increases, that would indicate a tendency of the dynamics toward a chaotic at-

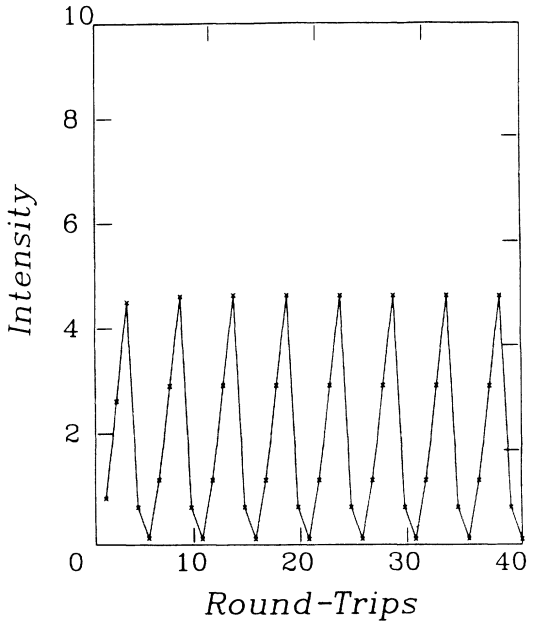

FIG. 6. Output intensity vs number of round-trips with $\tilde{\Delta}=-8$, $I_{in}=110$, $F=\infty$, $\phi_L=0.4$. See Fig. 5.

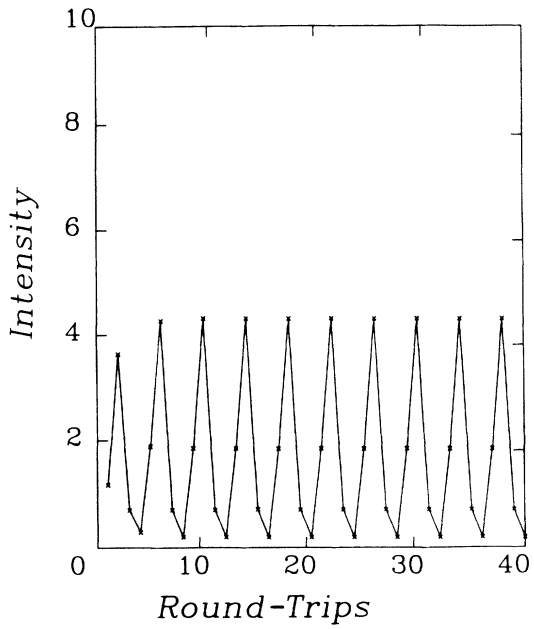

FIG. 7. Same as Fig. 6 with $I_{in}=150$.

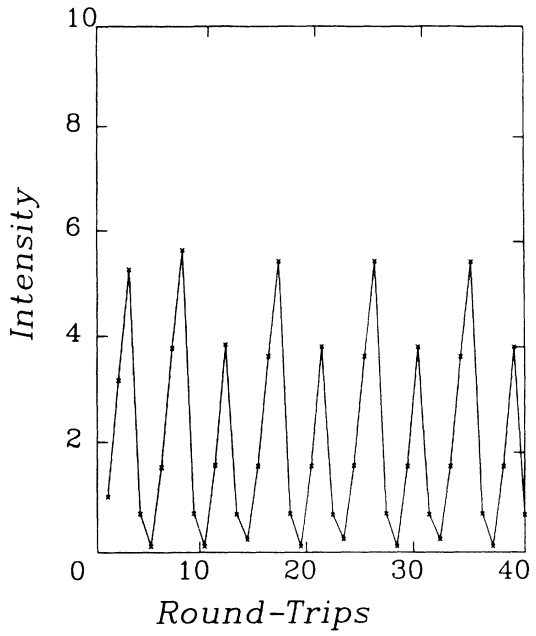

FIG. 8. Same as Fig. 6 with $I_{in}=130$.

tractor. On the contrary, we find that the dispersive coefficient is always smaller than the absorption coefficient, as we pointed out earlier. In view of the fact that the same effect of overlap between neighboring periods is found in Refs. 7, 8, and 15, where dispersive effects are not introduced, we can only attribute this effect to the ability of the oscillator, at those intensities, to respond in an ambivalent manner. That is, as the feedback pushes the input to higher values, sometimes it may be just enough to clear the turning point A in Fig. 1, and as the dynamics develops, it may have such magnitude as to overshoot the turning point considerably, and induced absorption would remain the dominant mechanism for the bistability. Only if the rays are allowed to couple do we have many periods that must coexist, as in the case of a Gaussian input.

The behavior we have examined in this section cannot completely reveal the complexity of the entire dynamics. We have found a complicated periodic dynamics, but it is not chaotic. We have only been able to explore a small range of the parameter space, these include the laser-atom detuning, cavity detuning, mirror reflectivity, and sample length. All of these parameters are important; the output intensity is sensitively dependent on the precise parameters that we use.

The higher periods in the output characteristics appear for lower input intensities and for the transverse profile this means that there will be sharp discontinuities in the intensity profile. That is, a Gaussian input will contain many intensities off the axis and if each such intensity has a characteristic oscillation period, diffraction will definitely play a major role in the determination of the new profiles. The diffractive coupling will tend to smooth the boundary regions. This brings up the question of whether or not the combination of transverse effects with these coexisting periodic characteristics will lock together to form a single period or a chaotic output. To answer this query the transverse effects are discussed in Sec. IV.

IV. RESULTS II: TRANSVERSE EFFECTS

An important parameter from previous studies of extrinsic optical bistability is the Fresnel number F which was introduced in Eq. (5). It determines the transverse coupling of the wave and will mix together plane-wave solutions that would tend towards different periodic solutions, as discussed in Sec. III. The numerical solution of the propagation equation involves fast-Fourier-Transform (FFT) methods and are extensively discussed in previous references.[13,14] The FFT algorithm includes many plane-wave modes in a simple manner and is an efficient algorithm. In our studies, we use a single transverse dimension. We sampled 128 points along the transverse coordinate, with a sampling interval $\Delta x=0.1$. We remark that cylindrical symmetry with two transverse dimensions can be performed with a quasi-fast-Hankel-transform.[16] Because we treat only one transverse dimension, comparison with future experiment would have to be qualitative. We draw from experience on two-dimensional modeling of extrinsic optical bistable devices.[17] The thresholds are affected, but the qualitative results are identical. Even an array of these devices can be studied to obtain critical separation distances for independent operation of each device in the array.[17,18]

The input beam is a Gaussian of unit width, where the field is

$$E(x)=E_0e^{-x^2},$$

or equivalently, the intensity is

$$I(x)=(E_0e^{-x^2})^2 . \tag{18}$$

The oscillator dynamics becomes increasingly more difficult to follow as the Fresnel number takes on finite values. F essentially determines the diffraction angle for each of the rays present on the Gaussian input. If F is large, only adjacent rays will couple and, to some degree, interfere with each other. If the rays are allowed to propagate over larger distances, then, eventually more rays are made to couple and the interference pattern will change.

If the nonlinear medium is in a ring-cavity configuration, the rays will couple in a substantially different way for each subsequent pass after the input intensity is turned on, since the phases change due to the interference between the waves and their interaction with the medium; the interference observed at the output side will progressively change, until a steady state is achieved. In order to illustrate this, we turn our attention to Fig. 9, where we consider propagation of a Gaussian beam in free space with its central part removed. This is equivalent to placing an opaque object in front of the beam, and letting the wave propagate beyond it. The result is that, unlike the full Gaussian beam, where degradation of the intensity is spatially smooth, the sharp

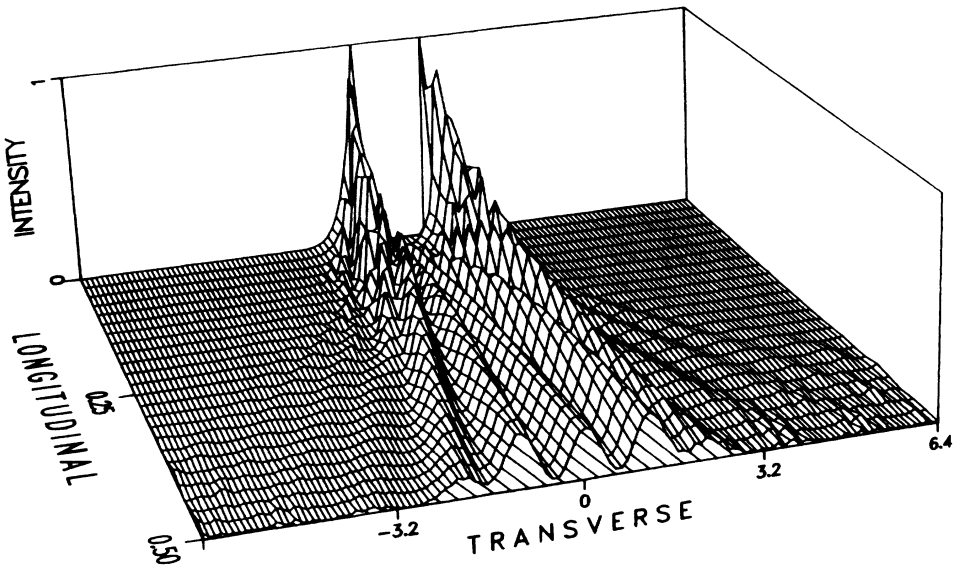

FIG. 9. Free space propagation of a Gaussian beam of unit width with $F=1$, and the central region blocked by an opaque strip at $z=0$. In this case, $F=2kd^2$, where k is the average wave vector of the packet, d is the width at half maximum, and the length is unity.

edges will produce much enhanced ray bending and a characteristic diffraction pattern will appear, just as in the Poisson spot case.

This in effect mimics the situation with the nonlinear oscillator medium. In a noncavity case, if the on-axis input intensity is set just above the turning point A in Fig. 1, then the central part of the beam is strongly absorbed, creating those sharp edges that so much favor diffractive coupling. In a cavity configuration, a slight change in the diffraction angle will drastically change the view from the output side, as pointed out earlier. Therefore one would expect that the output intensity sensitivity to the Fresnel number is drastically enhanced and completely unpredictable. In addition, the sharp discontinuities in the intensity present within the medium further enhance diffraction, thus complicating the prediction process. This in effect renders the plane-wave analysis inconsistent. A hybrid experiment such as the one outlined above cannot adequately describe the dynamics of an intrinsically bistable system.

Since it is practically impossible to scan the Fresnel number space in a continuous manner, we content ourselves with a few values that will hopefully help to extract the important physical characteristics of the system. In what follows the on-axis intensity $|E_0|^2=20$, the laser detuning $\tilde{\Delta}=-4$ and the Fresnel number will vary, so that qualitative differences may be made to appear for the same input parameters as diffraction becomes increasingly important.

In Fig. 10 we plot the output intensity profile at a particular moment in the evolution for $F=\infty$. The oscillations on the central axis of the beam are period 4. The off-axis input intensity has higher periods of oscillation, depending on the input intensity at each point according to the input intensities shown in Fig. 4. They oscillate independently and each intensity has a period whose value is the same as found by the plane-wave analysis of Sec. III. Even though the rays oscillate independently of each

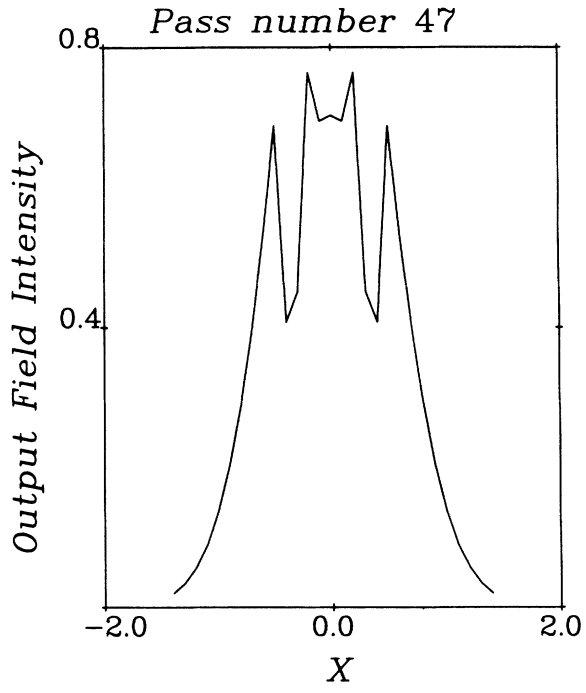

FIG. 10. Output intensity vs transverse coordinate as viewed at the output side with $\tilde{\Delta}=-4$, $F=\infty$ (no coupling case), $\phi_L=0.4$; the 47th pass through the medium is chosen.

other, we again point out that the threshold intensity is unchanged, but that settling of the oscillations to a specified period will take longer for off-axis rays, since some intensities are closer to threshold values.

Figure 11 shows the on-axis output intensity as a function of the number of round trips in the cavity for $F=1000$. Qualitative differences already begin to appear. As diffraction is not yet very important, it does nevertheless affect the central part of the beam by removing enough energy from it to require eighteen round-trips to complete a cycle, as opposed to four for $F=\infty$. Even though the central part of the beam has settled rather quickly, we observed that at the output mirror the situation is rather complicated. As only adjacent rays begin to couple, some parts of the beam will oscillate under their mutual influence. The whole beam eventually settles to a definite period of oscillation; again, we contrast this with the behavior for $F=\infty$, where different transverse regions have a different period. Figure 12 is an example of the output intensity at a particular time.

In order to establish the importance of diffraction for a specific Fresnel number we adopted the following criteria. First we looked at the width of the beam at half maximum at the output side and compared it to the original input Gaussian; second we looked for secondary maxima in the wings, which are the trademark of a diffracting beam. Even though only adjacent rays couple, we can safely assume that the $F=1000$ case is relatively diffraction-free, i.e, the input beam width is the same as the output beam width (see Fig. 12). The numerous peaks that appear in the center of the figure are due to the oscillator dynamical instabilities; at the boundary between different periods in the transverse direction, diffraction is important to synchronize all the periods together. We note that the outer wings of the beam are smooth and unaffected by diffraction effects in the center.

For $F=100$ the whole beam is locked into an oscillation of period 2. We find that this is neither self-focusing nor a waveguiding effect[6] on the electromagnetic energy.

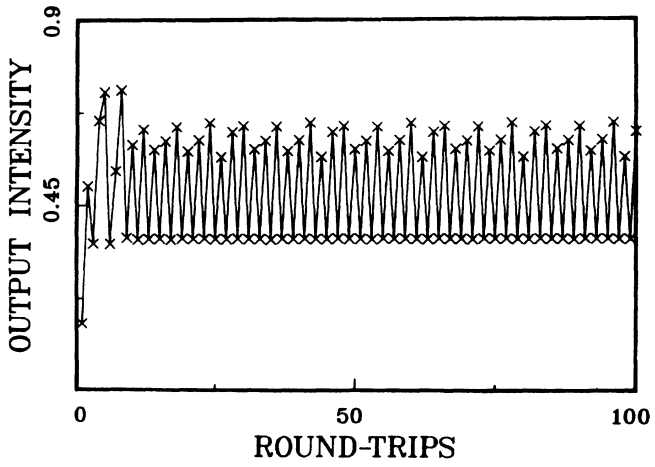

FIG. 11. On-axis output intensity vs number of round-trips with $F=1000$.

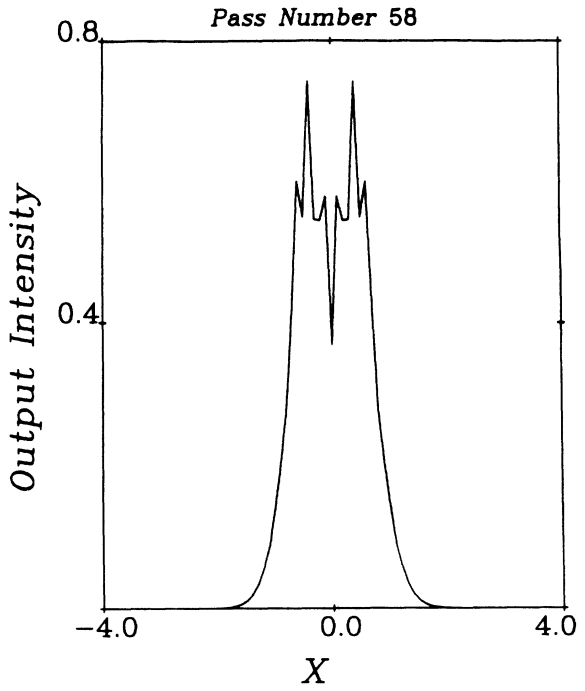

FIG. 12. Same as Fig. 10 with $F=1000$. Now pass number 58 has been chosen.

Diffraction at a sharp boundary is responsible for this, as in Fig. 9. As diffraction may now be relatively important, energy is redistributed to every part of the beam, even the outer portion of the output intensity profile. Figure 13 displays the transverse intensity profiles at the exit mirror. We find that the whole beam switches between these two states, which means that diffraction has caused just enough interference so that every part of the beam is locked into this final state. This situation could not have been predicted *a priori* for intermediate values of the Fresnel number. In this case secondary diffraction maxima are clearly visible at the outer fringe of the intensity profile.

For $F=5$ diffraction has definitely taken on a dominant role for the whole beam. The time dependence of the on-axis intensity, even though still periodic, has completely changed with respect to the plane-wave case. As rays couple strongly along the transverse coordinate, the whole beam tends towards a complex periodic structure. The wings of the transverse intensity profile are now forced to receive more energy from the center of the beam, and vice versa. Since the coupling is strong it is again difficult to make predictions, and the output will be rather complicated, as Fig. 14 shows. Again we find that the whole beam is locked into an oscillation period, in this case period 8. This is an important observation, since in this case it is clear that the presence of a large number of periods for plane-wave amplitudes (Fig.4), couple to give a completely stable profile at all Fresnel numbers that we have studied and furthermore, the number of periods is sensitive to the value of F. For $F=5$, a rudimentary ring structure is seen to appear and to ex-

tend to relatively large radius off the axis.

For the $F=1$ case, not shown here, diffraction is the dominant effect and steady state is quickly achieved within only a few round trips. Transverse coupling redistributes the energy and does not allow the system to build up an intensity profile that would give rise to any of the instabilities discussed above.

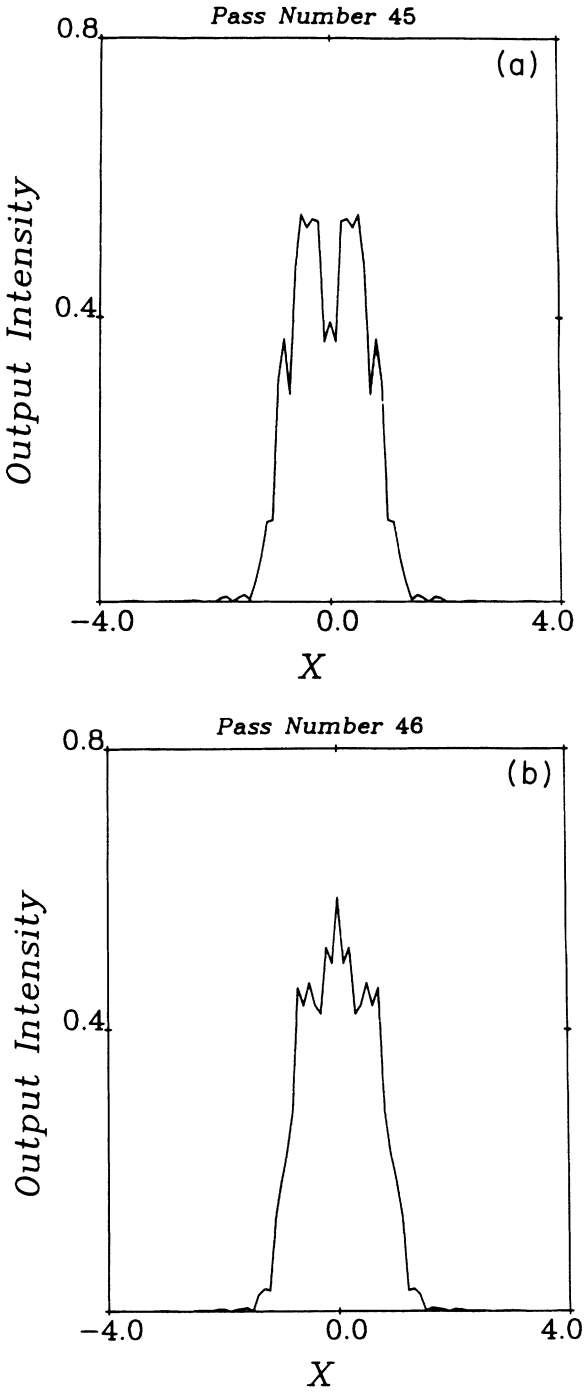

FIG. 13. Output intensity vs transverse coordinate with $F=100$. Pass numbers 45 and 46, labeled (a) and (b), respectively.

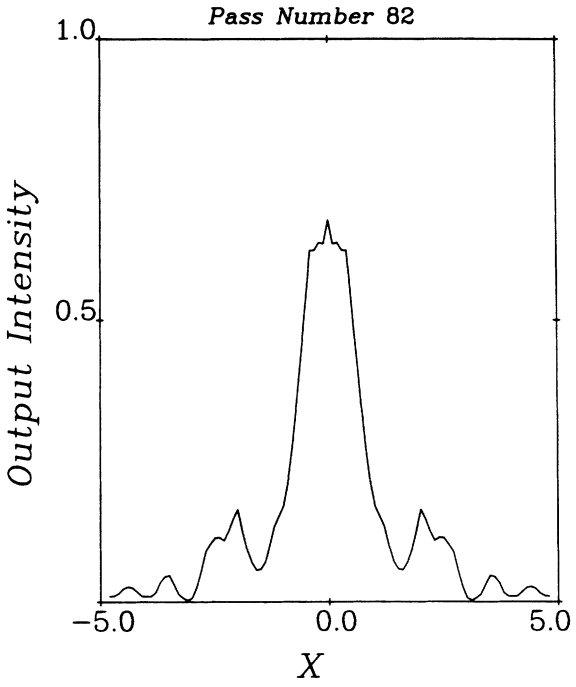

FIG. 14. Output intensity vs transverse coordinate with $F=5$. Pass number 82.

V. CONCLUSION

In conclusion, a medium modeled by anharmonically bound electrons has been analyzed. We find that the type of instabilities that exist in the plane-wave limit persist in the low Fresnel number regime, but the output beam profile is considerably complicated by diffractive coupling, allowing a time-dependent ring structure to develop out to large radius. Absorption effectively suppresses dispersive effects and chaos along with it, even far away from resonance, as well as, close to resonance. For fixed detuning, close to resonance, instabilities develop with a definite period of oscillation.

Chaotic output could be achieved by introducing a finite relaxation time of the material; the problem is then similar to the classical driven nonlinear oscillator model. It is also conceivable that chaotic behavior might be stimulated if the right set of parameters is used. In scanning Fresnel number space, we confirmed that the period of the output intensity's variations is very sensitive to this parameter. We also found that for some periods, such as 250 or 500, the steady state is preceded by an unusually long period of transients, which led us to believe that for some combination of the medium length, Fresnel number, cavity and laser detunings, the medium might never recover and display chaos.[19] Yet, we were not able to find such a window in parameter space.

As the detuning is increased, a Farey-tree-like structure appears, but only two oscillation modes are found to coexist. For the same input intensity, the whole beam locks onto a different period by simply changing the

Fresnel number, so that no Farey tree can be deduced for this case.

Finally we point out that, even though no originality is claimed on the model, the nonlinear oscillator can be a very useful generic model for the study of transverse effects in intrinsically bistable media, which to our knowledge have not been the object of a concentrated effort to date. The model is applicable to molecules which are driven near a vibrational resonance by a strong laser field,[20] and nanometer size metal particles that are driven near their surface plasmon resonance.[21] The model serves as a prototype for intrinsic optical bistability that naturally lends itself to further investigation.

ACKNOWLEDGMENTS

This research was performed with partial support from the U.S. Army Research Office, Department of the Army Contract No. DAAL03-D-001 and the National Science Foundation Grant No. ECS-8813028.

[1]W. J. Firth, I. Galbraith, and E. M. Wright, J. Opt. Soc. Am. B **2**, 1005 (1985); D. L. Wearie, J. P. Kermode, and V. M. Dwyer, Opt. Commun. **55**, 223 (1985); *Optical Bistability III,* edited by H. M. Gibbs, P. Mandel, N. Peyghambarian, and S. D. Smith (Springer, Berlin, 1986), p. 193ff and references therein; L. A. Lugiato and C. Oldano, Phys. Rev. A **37**, 3896 (1988).

[2]W. J. Firth and E. M. Wright, Opt. Commun. **40**, 233 (1982).

[3]J. V. Moloney, F. A. Hopf, and H. M. Gibbs, Phys. Rev. A **25**, 3442 (1982); W. J. Firth and C. Paré, Opt. Lett. **13**, 1096 (1988) and references therein.

[4]J. A. Goldstone and E. Garmire, Phys. Rev. Lett. **53**, 910 (1984).

[5]J. W. Haus, L. Wang, M. Scalora, and C. M. Bowden, Phys. Rev. A **38**, 4043 (1988).

[6]M. Scalora and J. W. Haus, J. Opt. Soc. Am. B **6**, 1714 (1989).

[7]M. Lindberg, S. W. Koch, and H. Haug, J. Opt. Soc. Am. B **3**, 751 (1986).

[8]M. Wegener and C. Klingshirn, Phys. Rev. A **35**, 1740 (1987).

[9]F. P. Mattar and C. M. Bowden, Phys. Rev. A **27**, 345 (1983).

[10]M. Lax, W. H. Louisell, and W. McKnight, Phys. Rev. A **11**, 1365 (1975).

[11]L. A. Lugiato and R. Lefever, Phys. Rev. Lett. **58**, 2209 (1987).

[12]H. J. Carmichael, R. R. Snapp, and W. C. Schieve, Phys. Rev. A **26**, 3408 (1982); J. W. Haus, C. M. Bowden, and C. C. Sung, J. Opt. Soc. Am. B **1**, 742 (1984).

[13]M. D. Feit and J. A. Fleck, Jr., Appl. Opt. **17**, 3990 (1978).

[14]J. V. Moloney, M. R. Belic, and H. M. Gibbs, Opt. Commun. **41**, 379 (1982).

[15]M. Wegener and C. Klingshirn, Phys. Rev. A **35**, 4247 (1987).

[16]A. E. Siegman, Opt. Lett. **1**, 13 (1977) and references therein.

[17]H. Richardson, E. Abraham, and W. J. Firth, Opt. Commun. **63**, 199 (1987).

[18]E. Abraham, Opt. Lett. **11**, 689 (1986).

[19]M. Scalora, J. W. Haus, and C. M. Bowden, in *Proceedings of the Conference on Coherence and Quantum Optics 6, Rochester, 1989,* edited by J. H. Eberly, L. Mandel, and E. Wolf (Plenum, New York, in press).

[20]C. Flytzanis and C. L. Tang, Phys. Rev. Lett. **45**, 441 (1980).

[21]J. W. Haus, N. Kalyaniwalla, R. Inguva, and C. M. Bowden, J. Appl. Phys. **65**, 1420 (1989); J. W. Haus, N. Kalyaniwalla, R. Inguva, M. Bloemer, and C. M. Bowden, J. Opt. Soc. Am. B **6**, 797 (1989).